Sensors and Actuators A 249 (2016) 269–275

Contents lists available at ScienceDirect

Sensors and Actuators A: Physical

journal homepage: www.elsevier.com/locate/sna

Development of flexible multi-channel muscle interfaces with advanced sensing function

Jiahui Wang[a,b,c], Zhuolin Xiang[a,b,c], Gil Gerald Lasam Gammad[a], Nitish V. Thakor[a,b], Shih-Cheng Yen[a,b,c,*], Chengkuo Lee[a,b,c,*]

[a] Department of Electrical & Computer Engineering, National University of Singapore, 4 Engineering Drive 3, 117576, Singapore
[b] Singapore Institute for Neurotechnology (SINAPSE), National University of Singapore, 28 Medical Drive, 117456, Singapore
[c] Center for Intelligent Sensors and MEMS, National University of Singapore, 4 Engineering Drive 3, 117576, Singapore

ARTICLE INFO

Article history:
Received 1 February 2016
Received in revised form 23 May 2016
Accepted 30 July 2016
Available online 2 September 2016

Keywords:
Muscle interface
Muscle fatigue
Flexible
Multi-channel
Electrical stimulation
pH monitoring

ABSTRACT

Functional Electrical Stimulation (FES) helps individuals with paralysis recover their muscle function. As opposed to voluntary muscle movement, which involves probabilistic recruitment of different muscle fibers at the neuromuscular junction, FES is usually performed using electrodes with just one channel, and as a result, tends to stimulate the same muscle fibers repeatedly. This induces excess muscle fatigue, which manifests itself as a loss of generated force after extended stimulation. Since the force generated is not typically measured in a FES system, electrical stimulation parameters need to be adjusted manually when muscle fatigue occurs. To address the problems of current FES, we propose a flexible muscle interface device with multiple stimulation electrodes and an integrated pH sensor. By using different subsets of electrodes for stimulation, alternating excitation of muscle fibers can be achieved to reduce fatigue in the muscles. At the same time, the pH sensor helps to provide quantified information about the state of the muscles, potentially allowing the stimulation parameters to be altered in a closed-loop fashion. Different interfacing materials were compared in terms of impedance and charge delivery ability. IrOx exhibited lower impedance of 0.7 kΩ at 1 kHz, and higher charge storage capacity (CSC) of 23.77 mC/cm^2. In *in vivo* muscle stimulation experiments, the use of alternating electrodes during stimulation induced less muscle fatigue, as well as less pH change, compared to using fixed electrode pairs. This flexible multi-channel stimulation device can potentially be used to reduce and monitor muscle fatigue during functional electrical stimulation.

1. Introduction

Paralysis is the loss of ability for a muscle or a group of muscles to move voluntarily. It is often caused by stroke and spinal cord injury, after which the voluntary movement of muscles is lost due to the inability of the brain to communicate with the corresponding muscles. Functional Electrical Stimulation (FES) is often used for individuals with paralysis to recover voluntary movement of muscle, by applying electrical stimulation to excitable muscles [1–5].

Currently, three kinds of muscle stimulation interfaces are commonly used: transcutaneous [6–8], percutaneous [9–11], and implanted interface [12–14]. The main advantage of transcutaneous stimulation is that it is non-invasive and easy to apply, but it has difficulty reaching deep muscles and selectively activating specific muscles. This is because when the electrical field is generated by the transcutaneous interface device, it spreads in the cutaneous layer, and will often activate other muscles along with the targeted muscle. It may also activate cutaneous pain receptors and cause pain in the subject. Percutaneous stimulation involves inserting needle electrodes through the skin to stimulate the underlying muscles. It has the ability to target deeper muscles, as well as isolating muscles for stimulation, but some subjects may be uncomfortable with the use of these needles, and improper sterilization of the needles or skin may result in infections that are hard to manage. Stimulation through wireless implanted devices requires surgery, and is thus the most invasive. However, once implanted, the devices can be powered and controlled transcutaneously through the skin,

* Corresponding authors at: Singapore Institute for Neurotechnology (SINAPSE), National University of Singapore, 28 Medical Drive, 117456, Singapore.
E-mail addresses: shihcheng@nus.edu.sg (S.-C. Yen), elelc@nus.edu.sg (C. Lee).

http://dx.doi.org/10.1016/j.sna.2016.07.034
0924-4247/

providing a safe interface that can be used repeatedly to stimulate deep muscles, as well as isolated muscles.

Implantable interfaces for FES have been developed for decades, but significant drawbacks still remain. The critical problem is that FES induces excessive fatigue. FES tends to activate muscle fibers simultaneously [15], and the activated muscles fibers are random [16,17]. In this way, FES induces muscle fatigue easily, and is different from normal voluntary muscle contraction, which has two mechanisms to lower fatigue [18]: one is to activate smaller and fatigue-resistant fibers first to delay the onset of fatigue [19,20]; another is to recruit fibers in an unsynchronized pattern to replace the fatigued fibers with others. Currently, most FES devices are unable to quantify the force generated through the muscle stimulation, so when fatigue sets in, the adjustment of the stimulation parameters needs to be made manually by experienced clinicians.

Till now, researchers have not reached a consensus on the chemical releasing mechanism that leads to muscle fatigue, and fascial muscle pH value may be an indicator of muscle fatigue. Some researchers agree that accumulated lactate leads to muscle fatigue [21]. While others agree that muscle fatigue is related to energy supply, under which circumstances faster expenditure of ATP than generation of ATP releases NH3 and monophosphate into blood [22].

In recent years, implantable devices based on flexible polymer substrates have started to emerge. These devices have been applied in other fields, including a 3D membrane for cardiac monitoring and stimulation [23], foldable electrode array for brain activity mapping [24], adaptive neural ribbon electrode for small nerve recording [25], instrumented surgical sutures for wound monitoring and therapy [26], and absorbable silk device for infection abatement [27].

The flexible polymer substrates, together with the usage of inert metal (gold) or absorbable metal (magnesium) as conductive layer, have been shown to be biocompatible as well [28–30]. The integration of different sensors and actuators, including electrical stimulation sites, electrical recording sites, temperature sensor, strain sensor, and micro-heater, makes these devices applicable for healthcare monitoring and functional stimulation. Unlike previous bulky implantable devices, these devices are flexible, so that they can conformably attach to target nerves, tissues, or organs for better recording and stimulation.

To address the problems of FES interfaces mentioned above, and take advantage of the development of multi-functional, implantable devices based on flexible substrates, we propose a flexible multi-channel muscle interface to reduce muscle fatigue and monitor pH to reflect muscle fatigue during FES. By alternating the stimulation electrode site pairs during FES, different muscle fibers located on the same muscle are excited alternatively, to mimic the voluntary muscle contraction pattern. Meanwhile, the IrOx pH sensor on the implanted interface monitors pH change to quantify the degree of muscle fatigue, so that corresponding adjustments on the stimulation parameters can potentially be made.

2. Design and fabrication

Fig. 1 shows the design of the muscle interface device. Six rectangular electrode pads were designed to fit a flexible printed circuit (FPC) connecter. Every electrode pad was connected to one electrode site with interconnects of 50 μm width. We designed the electrode site to be as large as possible to provide lower impedance (so as to consume less power during electrical stimulation) and to generate less heat during electrical stimulation. However, due to the limitation in device size, 600 μm was chosen as the electrode site diameter. Suture holes were designed to facilitate the fixation of the device on the target muscle with surgical suture.

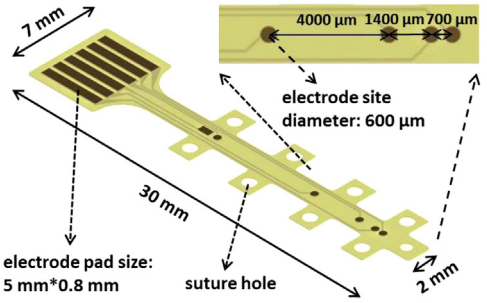

Fig. 1. Schematic illustration of device design. Six electrodes of same diameter are distributed with uneven distance between each other. Two arrays of suture holes facilitate the fixation of the device on the target muscle.

All chemicals were used directly after purchasing, without further purification. The chemicals were: Durimide 7500, Durimide developer HTRD-2, and RER 600, purchased from Fujifilm; AZ 9260, and AZ developer AZ 400 K, purchased from MicroChemicals; potassium carbonate, iridium chloride, and oxalic acid, purchased from Alfa Aesar.

As shown in Fig. 2, the fabrication of the sandwich-structure muscle interface started from a silicon wafer with a 200 nm aluminium layer. First, polyimide was spin coated, patterned with UV lithography, developed, and cured at 200 °C in N_2 to form the bottom layer (Fig. 2 (b)). The middle metal layer was realized by a liftoff process. The AZ layer was spin coated, UV pattered, and developed to generate the metal layer pattern. Two layers of 10 nm chromium and 200 nm gold were deposited by electron beam evaporator subsequently. Then, the liftoff process in acetone removed the extra Cr/Au by dissolving the AZ layer, and left the desired metal pattern on the device (Fig. 2 (c)). A top polyimide layer was fabricated using the same method as the bottom layer.

IrOx was coated on the electrode sites, to be used as electrical stimulation and pH monitoring material. The electroplating solution was prepared in the following way: 300 mg iridium chloride was dissolved in 200 ml DI water, and stirred for 15 min. Then, 1000 mg oxalic acid powder was added to the solution, and stirred for 10 min. To adjust the pH to 10.5, potassium carbonate was slowly added to the solution. The prepared solution sat at room temperature for 2 days before use, during which it turned into a violet color. It was stored in a dark bottle at 4 °C in the fridge until it was used.

To electroplate the electrode sites with IrOx, the electrode pads were connected to the negative terminal of an external voltage source, with only the electrode sites immersed in the prepared solution. The positive terminal of the external voltage source was connected to a platinum mesh electrode immersed in the solution. Pulsed voltage, with peak-to-peak magnitude of 3 V and bias voltage of 1.5 V, was applied for 3 min to plate IrOx.

The device was then released from the substrate, by dissolving the Al sacrificial layer, as described previously [31]. The silicon substrate and platinum mesh electrode were immersed in a conductive solution of 2 M NaCl. The wafer was connected to the positive terminal of the external voltage source, and the platinum mesh electrode was connected to the negative terminal. DC voltage of 1 V was applied for 15 min, and then raised to 15 V for another 3 h. The released device is shown in Fig. 2 (f).

Fig. 3 shows the connection between the muscle interface device and a FPC connector. Since the muscle interface was designed to fit the FPC connector, it inserted into the opened FPC connector easily, with an additional spacer used to ensure good contact.

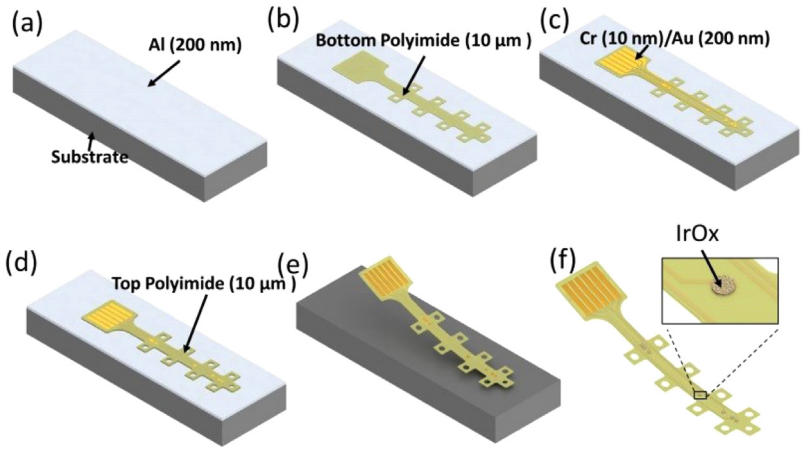

Fig. 2. Fabrication process. The device is fabricated layer by layer on the silicon substrate, and then released by etching away the aluminium sacrificial layer.

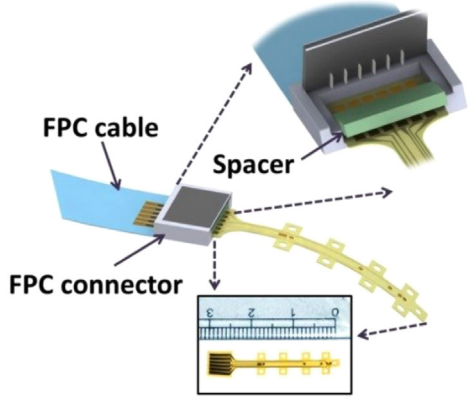

Fig. 3. Schematic illustration of the device connected to a FPC connector. The pads on the device are designed to match the FPC connector, and can be plugged in the FPC connector easily.

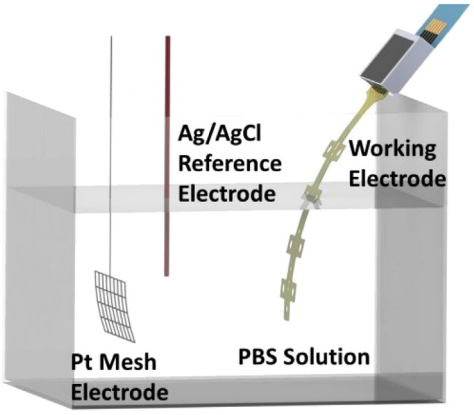

Fig. 4. Three-electrode setup. The working electrode, Ag/AgCl reference electrode, and Pt mesh electrode are immersed into the PBS solution.

3. Electrical characterization

3.1. Electrical characterization of stimulation interface

Cyclic voltammetry (CV), electrochemical impedance spectroscopy (EIS), and potential transient responses were measured for electrode sites of three different materials (Au, Pt black, and IrOx) on 600 μm-diameter electrode sites, to characterize the performance of the stimulation electrode and the properties of the IrOx. Au was the initial conductive layer grown by sputtering, while Pt black and IrOx were electroplated separately to modify the contact surface.

The measurements were performed using a three-electrode setup: the electrode to be measured acted as the working electrode, a Ag/AgCl electrode acted as the reference electrode, and a Pt mesh acted as the counter electrode (Fig. 4). These three electrodes were immersed into phosphate-buffered saline (PBS) solution (pH = 7).

In the measurement of CV and EIS, the working electrode, Ag/AgCl reference electrode, and the Pt counter electrode were all connected to the potentiostat (Autolab M204). However, in the measurement of CSC, the Pt mesh electrode was connected to both the oscilloscope (Keysight, 2000 X-Series) and a custom made current stimulator, while the Ag/AgCl reference was connected to the other terminal of the oscilloscope and the working electrode was connected to the other terminal of the current stimulator.

Fig. 5 shows the CV measurement results. The closed area formed by each curve represents the charge storage capacity (CSC)

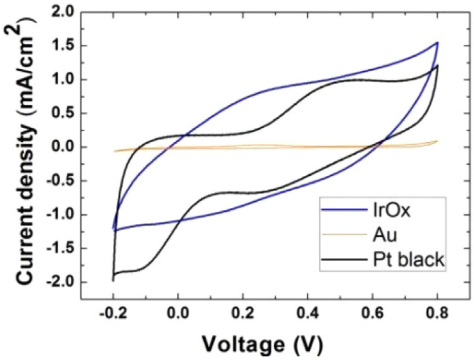

Fig. 5. Cyclic Voltammograms (CV) of different contact materials. The current density is derived from dividing the current by interface electrode area.

of the material. In this area, a reversible redox reaction occurred, which indicated that the coating material on the electrode surface was not dissolved in the solution. By using Eq. (1), where the voltage sweep rate was 50 mV/s, the CSC of each material was calculated. IrOx achieved the highest CSC of 23.7 mC/cm^2, in correspondence with previous results [32], and much higher than Au, which exhibited a CSC of 0.506 mC/cm^2. The higher CSC of IrOx means that it can deliver more charge to the tissue when used as a muscle stimulation interface material. As opposed to nerve stimulation, which only needs stimulation currents of several nA, muscle stimulation requires several mA of current. As a result, materials with higher

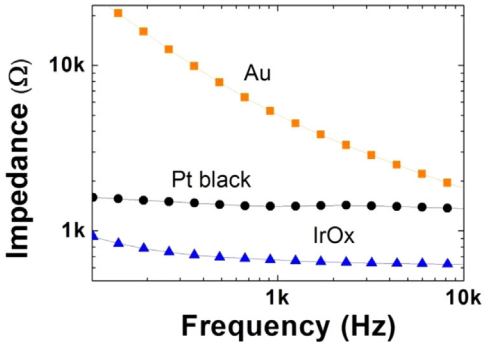

Fig. 6. Bode plot of electrode impedance. At 1 KHz, IrOx shows lower impedance of 0.7 kΩ, compared to Pt black of 1.4 kΩ and gold of 5.3 kΩ.

charge delivery capacity, which IrOx has demonstrated here, meet the requirements for muscle stimulation.

$$CSC = \frac{\int |Current \quad density| * d(Voltage)}{Voltage \quad sweep \quad rate} \tag{1}$$

Fig. 6 shows the complex impedance magnitudes for 600 μm-diameter electrode sites. At all frequencies below 10 kHz, IrOx showed lower impedance than Pt black and Au. At 1 kHz, the fundamental frequency of biological relevance in action potentials, the impedances of IrOx, Pt black, and Au were: 0.7 kΩ, 1.4 kΩ, and 5.3 kΩ, respectively. For the purposes of muscle stimulation, where high stimulation currents are used, lower impedances are critical as less heat will be generated. So, IrOx with its low impedance is preferred as the material of the stimulation electrodes.

Using the method described by Negi et al. [33], the maximum stimulation current was found by gradually increasing the stimulation current until the maximum negative potential excursion (Emc) reached the water reduction potential of −0.6 V, with stimulation pulse widths fixed as 120 μs. Using Eq. (2), the charge injection capacity was calculated. The comparison of CIC is shown in Table 1, where IrOx shows the highest CIC of 3.95 mC/cm^2. The reason for the difference between measured CIC and CSC for each material was that the measurements were performed at different frequencies. The CSC measurements were carried out at a frequency of 0.025 Hz, while the CIC measurements were carried out at 20 Hz. At the low frequency of 0.025 Hz, carriers have enough time to diffuse in the solution to finish the reversible reaction. While at higher frequencies, some carriers may not be able to reach the electrode before the onset of the next redox reaction, thus causing a lower deliverable charge in the reversible reaction.

$$CIC = \frac{Stimulation \quad current \times Pulse \ duration}{Electrode \quad site \quad area} \tag{2}$$

Compared to Pt black, IrOx showed improvements in both impedance and charge delivery ability. Apart from being used widely at the stimulation interface, IrOx is also widely used in pH sensing. As a result, we choose to use IrOx instead of Pt black as the coating material in our device.

3.2. Calibration of IrOx pH sensor

A commercial pH meter (Hach, LPV2550T.97.002) was used to calibrate the pH measurements with the IrOx electrode. The calibration was performed in solutions of different pH value, by mixing hydrochloric acid (HCl) and potassium hydroxide (KOH) solutions with different ratios. Before the measurement of each solution, the commercial pH meter, IrOx electrode, and Ag/AgCl reference electrode were rinsed in DI water and blown dry using N_2 gun.

For each prepared solution, the pH was first measured using the commercial pH meter, and then the IrOx electrode. When measured

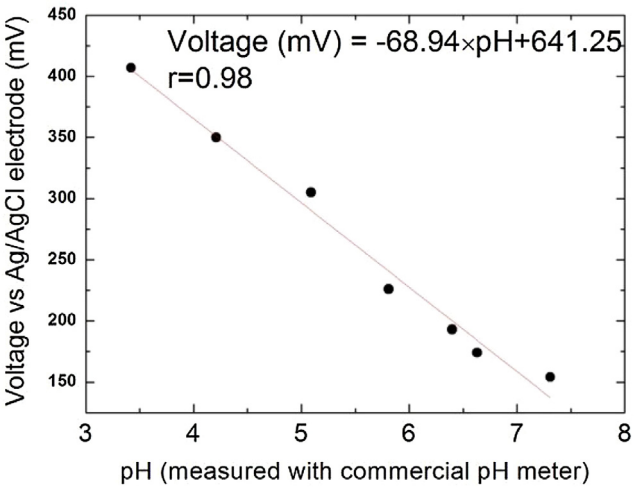

Fig. 7. pH calibration of IrOx electrode and commercial glass pH meter. Open circuit voltage shows linear relationship with the pH change.

with the IrOx electrode, both the IrOx electrode and Ag/AgCl reference electrode were immersed in the solution, and connected to the multi-meter (Fluke 45) for voltage readout. We waited fifteen seconds between readings to ensure that we obtained stable readouts of the Open Circuit Voltage (OCV) between the IrOx electrode and Ag/AgCl reference electrode.

The pH calibration result is shown in Fig. 7. The IrOx electrode was tested in solutions with lower pH at first, and then in solutions with higher pH, and repeated again from higher pH to lower pH. The mean value of the OCV readout in the same solution was plotted. When pH decreased by 1, the voltage readout decreased by 68.94 mV. The correlation between the OCV and pH was computed before in-vivo measurements, so that the OCV readout during in-vivo tests could be mapped to pH values.

4. In-vivo muscle fatigue measurement

4.1. Study on stimulation parameters

All procedures were performed in accordance with the ethics guidelines of the Agri-Food and Veterinary Authority of Singapore and approved by the Institutional Animal Care and Use Committee at the National University of Singapore. Male Sprague-Dawley rats were anesthetized with isoflorane, and isoflorane vapor was continuously supplied to maintain the rat under anesthesia during the experiment.

Muscle stimulation was performed on both legs of the same rat, first on the right leg, followed by the left. The biceps femoris muscle, right underneath the skin layer, was chosen as the target muscle. The skin on the right leg was cut with a blade, and fat on the muscle was removed carefully with tweezers. After exposing the muscle, the motor unit of the biceps femoris muscle was found by identifying the position where maximum muscle contraction was generated. To fix the electrode to the motor unit, surgical sutures were made through suture holes to the muscle tissue, as shown in Fig. 8. To quantify muscle contraction under electrical stimulation, a pulley system was used: using a string, a 10 g weight suspended on a pulley at the edge of the table was tied to the ankle of the rat leg. Under electrical stimulation, the rat leg kicked backwards, and pulled the weight up, which was recorded by a video camera placed in front of the weight. By comparing the displacement of the weight, the contraction of the leg was quantified.

The electrical stimulation consisted of several signal pulse trains, with a time interval between each of the pulse trains. Within

Table 1
Comparison of impedance, CSC and CIC.

	1KHz impedance (KΩ)	Charge Storage Capacity (mC/cm^2)	Charge Injection Capacity (mC/cm^2)
IrOx	0.7	23.7	3.95
Pt black	1.4	21.42	2.96
Au	5.3	0.506	0.329

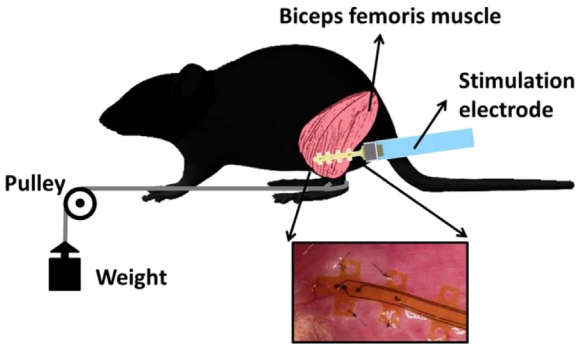

Fig. 8. Illustration of in-vivo muscle stimulation. The device is sutured to Biceps femoris muscle surface. A weight is tied to the leg through a pulley system. By recording the vertical movement of the weight, the leg displacement can be derived.

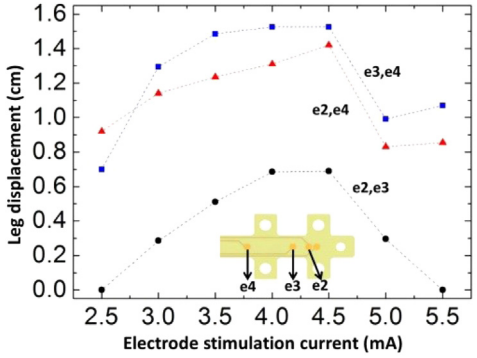

Fig. 9. Correlation between electrode stimulation current and leg displacement (mean value of 20 displacements). For a certain subset of electrode, the leg displacement tends to increase with the stimulation current at first, and then saturate, followed by dropping at large stimulation current.

each pulse train, multiple biphasic pulses were delivered. For a certain pair of electrode sites, several electrical stimulation parameters were studied: current magnitude (I), pulse width (w), stimulation frequency (f), pulse number (n) in a train of electrical stimulation, and time interval between two pulse trains of electrical stimulation ($T_{interval}$).

We first learnt from the experiment that changing pulse width and time interval between two pulse trains of electrical stimulation had a small influence on the induced muscle contraction magnitude. As a result, these two parameters were fixed during the study to w = 100 μs and $T_{interval}$ = 3 s.

Stimulation frequency and pulse number were optimized together to achieve smooth muscle contraction. When low stimulation frequencies were used, individual tetanus muscle contractions were observed, as the muscle fibers relaxed before the onset of the next stimulation pulse. When a small pulse number was used, very slight tetanus contractions were observed, as the muscle fibers were not able to accumulate enough force. Thus, the stimulation frequency and pulse number were fixed at f = 50 Hz and n = 20 per pulse train.

The result of using different electrode pairs and stimulation current is shown in Fig. 9. Here, we used D_{mn} to denote the leg displacement measured when using stimulation on electrode sites

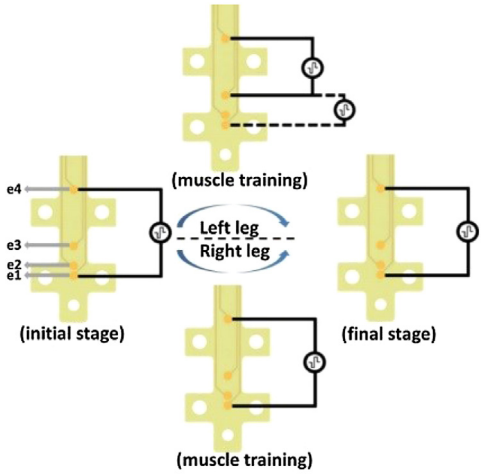

Fig. 10. Experiment design for comparison of muscle fatigue using different electrode pairs. During the muscle fatigue induce process, the left leg is stimulated with alternating electrode pairs, while the right leg is stimulated with fixed electrode pair.

m and n. Except for I = 2.5 mA, the relationship of leg displacement was: $D_{34} > D_{24} > D_{23}$. This can be explained with the mechanism of muscle contraction under electrical stimulation: when more muscle fibers are excited, larger contraction will be generated. For electrical stimulation on e2 and e3, since the distance between the electrode contact was small, a strong, localized electric field was created, and only a few muscle fibers were excited. For stimulation of e2 and e4, the electric field was distributed over a larger distance, so the charge at each location was reduced, resulting in fewer muscle fibers being activated. For stimulation of e3 and e4, a good balance of electrical field spread and localized magnitude was achieved, thus a larger portion of muscle fibers were excited. The sole exception occurred at I = 2.5 mA, where D_{24} was found to be larger than D_{34} even though the distance between e2 and e4 was larger than that between e3 and e4. This may be because the stimulation current was low, so the spread of the electrical field played a more important role than the magnitude of the electrical field.

When using the same electrode pair, another trend was observed: with increased stimulation current, the leg displacements reached saturation after a certain current magnitude. This suggests that smaller currents can be used to generate the desired displacement to protect the coating material on the electrode.

4.2. Muscle fatigue measurement

In the muscle fatigue experiments, the electrode was first implanted on the right leg, and then on the left leg of the same rat. For the right leg, muscle stimulation was performed continuously using the same electrode pair (e1 and e4) to induce muscle fatigue. For the left leg, muscle stimulation was performed by alternating the electrode pairs (e1 and e3, e3 and e4) to mimic the voluntary muscle contraction by exciting different muscle fibers.

The electrical stimulation for each leg was carried out in three stages, as shown in Fig. 10. In the initial stage, the OCV between the IrOx electrode and the external Ag/AgCl reference electrode (which was attached on the same muscle) was recorded. In the ini-

Table 2
Results of muscle fatigue comparison.

	Mean displacement (cm)		pH	
	Left leg	Right leg	Left leg	Right leg
Before stimulation	1.14	0.6	6.5	6.6
After stimulation	0.645	0.05	6.7	7.3

tial stage, a standard stimulation was applied to e1 and e4: I = 2 mA, f = 50 Hz, w = 100 μs, n = 20, $T_{interval}$ = 3 s. The weight displacement was measured using a pulley system over 20 muscle contractions. Then, muscle fatigue was induced in each group with a series of muscle stimulation trials. To induce muscle fatigue during muscle stimulation, a higher current magnitude of 4.5 mA was used, with other parameters kept the same as in the initial stage. In the final stage, the same standard stimulation was applied to the muscle again, and weight displacement was recorded. Right after the final stage, the OCV between IrOx electrode and the external Ag/AgCl reference electrode was recorded.

The comparison of muscle fatigue under different stimulation patterns is shown in Table 2. Mean displacement of 20 smooth contractions on the left leg (using alternating electrode pairs) reduced by 43.4%, while those on the right leg (using a constant electrode pair) reduced by 91.7%. This showed that muscle fatigue induced by alternating electrode pairs was lower than that with a constant electrode pair. Meanwhile, the pH change on the left leg was lower than that of the right leg.

The reduction of leg displacement was in correspondence with the reduction in pH change. It suggests that we may be able to quantify muscle fatigue by monitoring pH change. Since the electrical stimulation sites and pH recording sensor were integrated on the electrode, this suggests that closed-loop control of muscle stimulation may be possible for long-term implantation: when significant muscle fatigue is detected through a pH change, the stimulation current can then be increased before further muscle stimulation.

5. Conclusions

In this paper, we have described a muscle interface device with integration of multi-channel electrical stimulation and pH sensing. IrOx was employed as the electrode material, which exhibited lower impedance of 0.7 kΩ at 1 kHz, and higher CIC of 23.77 mC/cm^2. By mimicking voluntary muscle contraction, we showed that multi-channel stimulation produced less muscle fatigue. We also showed that with IrOx based pH monitoring on the surface of the muscle, closed-loop control of FES may be possible. The pH feedback signal may offer an indication of muscle fatigue, which will allow the device to automatically increase the stimulation current to achieve the same muscle contraction. This concept will be tested in future experiments.

Acknowledgements

This work was supported by grants from the National Research Foundation (NRF) CRP project "Self-Powered Body Sensor Network for Disease Management and Prevention Oriented Healthcare (NRF2011 NRF-CRP001-057)" (R-263-000-A27-281) and National Research Foundation (NRF) CRP project "Peripheral Nerve Prostheses: A Paradigm Shift in Restoring Dexterous Limb Function (NRF-CRP10-2012-01)" (R-719-000-001-281).

References

[1] E. Marsolais, R. Kobetic, Functional electrical stimulation for walking in paraplegia, J. Bone Joint Surg. 69 (1987) 728–733.
[2] M. Granat, A. Ferguson, B. Andrews, M. Delargy, The role of functional electrical stimulation in the rehabilitation of patients with incomplete spinal cord injury-observed benefits during gait studies, Spinal Cord 31 (1993) 207–215.
[3] G. Pfurtscheller, G.R. Müller, J. Pfurtscheller, H.J. Gerner, R. Rupp, 'Thought'–control of functional electrical stimulation to restore hand grasp in a patient with tetraplegia, Neurosci. Lett. 351 (2003) 33–36.
[4] A.E. Scremin, L. Kurta, A. Gentili, B. Wiseman, K. Perell, C. Kunkel, O.U. Scremin, Increasing muscle mass in spinal cord injured persons with a functional electrical stimulation exercise program, Arch. Phys. Med. Rehabil. 80 (1999) 1531–1536.
[5] P.D. Faghri, R.M. Glaser, S.F. Figoni, Functional electrical stimulation leg cycle ergometer exercise: training effects on cardiorespiratory responses of spinal cord injured subjects at rest and during submaximal exercise, Arch. Phys. Med. Rehabil. 73 (1992) 1085–1093.
[6] S. Mangold, T. Keller, A. Curt, V. Dietz, Transcutaneous functional electrical stimulation for grasping in subjects with cervical spinal cord injury, Spinal Cord 43 (2005) 1–13.
[7] D. Graupe, H. Cerrel-Bazo, H. Kern, U. Carraro, Walking performance, medical outcomes and patient training in FES of innervated muscles for ambulation by thoracic-level complete paraplegics, Neurol. Res. 30 (2008) 123–130.
[8] T. Keller, A. Kuhn, Electrodes for transcutaneous (surface) electrical stimulation, J. Autom. Control 18 (2008) 35–45.
[9] Y. Shimada, K. Sato, H. Kagaya, N. Konishi, S. Miyamoto, T. Matsunaga, Clinical use of percutaneous intramuscular electrodes for functional electrical stimulation, Arch. Phys. Med. Rehabil. 77 (1996) 1014–1018.
[10] K. Fujita, Y. Handa, N. Hoshimiya, M. Ichie, Stimulus adjustment protocol for FES-induced standing in paraplegia using percutaneous intramuscular electrodes, IEEE Trans. Rehabil. Eng. 3 (1995) 360–366.
[11] J.S. Knutson, G.G. Naples, P.H. Peckham, M.W. Keith, Electrode fracture rates and occurrences of infection and granuloma associated with percutaneous intramuscular electrodes in upper-limb functional electrical stimulation applications, J. Rehabil. Res. Dev. 39 (2002) 671–684.
[12] F. Sato, T. Nomoto, G. Kano, H. Matsuki, T. Sato, A new contactless power-signal transmission device for implanted functional electrical stimulation (FES), IEEE Trans. Magn. 40 (2004) 2964–2966.
[13] E. Hardin, R. Kobetic, L. Murray, M. Corado-Ahmed, G. Pinault, J. Sakai, S.N. Bailey, C. Ho, R.J. Triolo, Walking after incomplete spinal cord injury using an implanted FES system: a case report, J. Rehabil. Res. Dev. 44 (2007) 333.
[14] C. Ethier, E.R. Oby, M. Bauman, L.E. Miller, Restoration of grasp following paralysis through brain-controlled stimulation of muscles, Nature 485 (2012) 368–371.
[15] A. Carpentier, J. Duchateau, K. Hainaut, Motor unit behaviour and contractile changes during fatigue in the human first dorsal interosseus, J. Physiol. 534 (2001) 903–912.
[16] C.M. Gregory, C.S. Bickel, Recruitment patterns in human skeletal muscle during electrical stimulation, Phys. Ther. 85 (2005) 358–364.
[17] C.S. Bickel, C.M. Gregory, J.C. Dean, Motor unit recruitment during neuromuscular electrical stimulation: a critical appraisal, Eur. J. Appl. Physiol. 111 (2011) 2399–2407.
[18] P.H. Peckham, J.S. Knutson, Functional electrical stimulation for neuromuscular applications*, Annu. Rev. Biomed. Eng. 7 (2005) 327–360.
[19] M. Vanderthommen, J. Duchateau, Electrical stimulation as a modality to improve performance of the neuromuscular system, Exerc. Sport Sci. Rev. 35 (2007) 180–185.
[20] M. Jubeau, J. Gondin, A. Martin, A. Sartorio, N. Maffiuletti, Random motor unit activation by electrostimulation, Int. J. Sports Med. 28 (2007) 901–904.
[21] P. Tesch, B. Sjödin, A. Thorstensson, J. Karlsson, Muscle fatigue and its relation to lactate accumulation and LDH activity in man, Acta Physiol. Scand. 103 (1978) 413–420.
[22] K. Sahlin, M. Tonkonogi, K. Söderlund, Energy supply and muscle fatigue in humans, Acta Physiol. Scand. 162 (1998) 261–266.
[23] L. Xu, S.R. Gutbrod, A.P. Bonifas, Y. Su, M.S. Sulkin, N. Lu, H.-J. Chung, K.-I. Jang, Z. Liu, M. Ying, 3D multifunctional integumentary membranes for spatiotemporal cardiac measurements and stimulation across the entire epicardium, Nat. Commun. 5 (2014).
[24] J. Viventi, D.-H. Kim, L. Vigeland, E.S. Frechette, J.A. Blanco, Y.-S. Kim, A.E. Avrin, V.R. Tiruvadi, S.-W. Hwang, A.C. Vanleer, Flexible foldable, actively multiplexed, high-density electrode array for mapping brain activity in vivo, Nat. Neurosci. 14 (2011) 1599–1605.
[25] Z. Xiang, S.C. Yen, S. Sheshadri, J. Wang, S. Lee, Y.H. Liu, L.D. Liao, N.V. Thakor, C. Lee, Progress of flexible electronics in neural Interfacing—a self-adaptive non-invasive neural ribbon electrode for small nerves recording, Adv. Mater. 28 (2016) 4472–4479.
[26] D.H. Kim, S. Wang, H. Keum, R. Ghaffari, Y.S. Kim, H. Tao, B. Panilaitis, M. Li, Z. Kang, F. Omenetto, Thin, flexible sensors and actuators as 'instrumented'surgical sutures for targeted wound monitoring and therapy, Small 8 (2012) 3263–3268.
[27] H. Tao, S.-W. Hwang, B. Marelli, B. An, J.E. Moreau, M. Yang, M.A. Brenckle, S. Kim, D.L. Kaplan, J.A. Rogers, Silk-based resorbable electronic devices for remotely controlled therapy and in vivo infection abatement, Proc. Natl. Acad. Sci. 111 (2014) 17385–17389.
[28] R. Richardson, J. Miller, W.M. Reichert, Polyimides as biomaterials: preliminary biocompatibility testing, Biomaterials 14 (1993) 627–635.

[29] N. Lago, K. Yoshida, K.P. Koch, X. Navarro, Assessment of biocompatibility of chronically implanted polyimide and platinum intrafascicular electrodes, IEEE Trans. Biomed. Eng. 54 (2007) 281–290.
[30] J.-M. Seo, S.J. Kim, H. Chung, E.T. Kim, H.G. Yu, Y.S. Yu, Biocompatibility of polyimide microelectrode array for retinal stimulation, Mater. Sci. Eng.: C 24 (2004) 185–189.
[31] Z. Xiang, S.-C. Yen, N. Xue, T. Sun, W.M. Tsang, S. Zhang, L.-D. Liao, N.V. Thakor, C. Lee, Ultra-thin flexible polyimide neural probe embedded in a dissolvable maltose-coated microneedle, J. Micromech. Microeng. 24 (2014) 065015.
[32] S.J. Wilks, S.M. Richardson-Burns, J.L. Hendricks, D.C. Martin, K.J. Otto, Poly (3, 4-ethylenedioxythiophene) as a micro-neural interface material for electrostimulation, Front. Neuroeng. 2 (2009).
[33] S. Negi, R. Bhandari, F. Solzbacher, Morphology and electrochemical properties of activated and sputtered iridium oxide films for functional electrostimulation, Sci. Res. 2 (3) (2012).

Biographies

Wang Jiahui She received her B.S. degree from Department of Microelectronics at Fudan University in 2014. Currently, she is a PhD student at the Department of Electrical & Computer Engineering. Her research interest includes implantable neuromuscular interfacing and flexible wearable device.

Zhuolin Xiang He received B.Eng. degree from Department of Information and Electronics, Beijing Institute of Technology in 2011, and Ph.D degree from Department of Electrical & Computer Engineering, National University of Singapore in 2015. His research interests focus mainly on BioMEMS devices for drug delivery and neural interfacing.

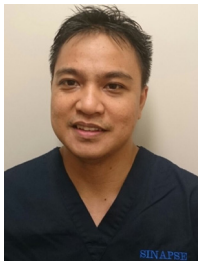

Gil Gerald Lasam Gammad Over 6 years of experience in laboratory animals focused on performing surgical procedures and veterinary care, and support for the research team. Multiple surgical experiences in multiple species which includes non-human primates, swine, rabbits and rodents in Contract Research Organization (Maccine Pte Ltd and Innoheart Pte Ltd) and at the National University of Singapore.

Shih-Cheng Yen He is an Assistant Professor, Department of Electrical and Computer Engineering, National University of Singapore. He received B.S.E., Department of Pennsylvania in 1993, M.S.E., Department of Bioengineering, University of Pennsylvania in 1993, and Ph.D., Department of Bioengineering, University of Pennsylvania in 1998. His research interests include neural coding, mechanisms underlying computation in the visual system, visual psychophysics, and biological models of the visual system.

Nitish V. Thakor He is the Director of Singapore Institute for Neurotechnology (SINAPSE) at National University of Singapore, as well as Professor of Electrical and Computer Engineering and Biomedical Engineering at NUS. His technical expertise is in the field of Neuroengineering, including neural instrumentation, neuromorphic engineering, neural microsystems, optical imaging of the nervous system, neural control of prosthesis and brain machine interface and cognitive engineering.

Chengkuo Lee He is an Associate Professor, Electrical & Computer Engineering, National University of Singapore. He received M.Sc., in Department of Materials Science & Engineer, National Tsing Hua University in 1991, and M.Sc., in Department of Industrial & System Engineering, the State University of New Jersey in 1993, and Ph.D., in Department of Precision Engineering, University of Tokyo in 1996. His research interest covers optical MEMS, bioMEMS, microfluidics, energy harvesting, and transdermal drug delivery.